LBL-23346
Preprint

Lawrence Berkeley Laboratory
UNIVERSITY OF CALIFORNIA

Materials & Chemical Sciences Division

RECEIVED
LAWRENCE
BERKELEY LABORATORY
JUN 9 1987
LIBRARY AND
DOCUMENTS SECTION

Submitted to the American Ceramic Society

EFFECT OF RIGID INCLUSIONS ON THE SINTERING OF GLASS POWDER COMPACTS

M.N. Rahaman and L.C. De Jonghe

April 1987

TWO-WEEK LOAN COPY
This is a Library Circulating Copy
which may be borrowed for two weeks.

LBL-23346 c.2

Prepared for the U.S. Department of Energy under Contract DE-AC03-76SF00098

DISCLAIMER

This document was prepared as an account of work sponsored by the United States Government. While this document is believed to contain correct information, neither the United States Government nor any agency thereof, nor the Regents of the University of California, nor any of their employees, makes any warranty, express or implied, or assumes any legal responsibility for the accuracy, completeness, or usefulness of any information, apparatus, product, or process disclosed, or represents that its use would not infringe privately owned rights. Reference herein to any specific commercial product, process, or service by its trade name, trademark, manufacturer, or otherwise, does not necessarily constitute or imply its endorsement, recommendation, or favoring by the United States Government or any agency thereof, or the Regents of the University of California. The views and opinions of authors expressed herein do not necessarily state or reflect those of the United States Government or any agency thereof or the Regents of the University of California.

EFFECT OF RIGID INCLUSIONS ON THE SINTERING OF GLASS POWDER COMPACTS

M. N. Rahaman[+*] and L. C. De Jonghe[*]

Materials and Chemical Sciences Division, Lawrence Berkeley Laboratory, University of California, Berkeley, California 94720

Abstract

The effect of rigid inclusions on the sintering of glass powder compacts has been investigated at 600°C. The densification rates show good agreement with the rule of mixtures for inclusion volume fractions of ≤0.1. The transient stresses generated during sintering by the presence of the inclusions were evaluated from the sintering data. Below inclusion volume fractions of ~0.12, the results are in excellent agreement with Scherer's theory for viscous sintering with rigid inclusions. At higher inclusion volume fractions, interactions between the inclusion particles lead to large deviations from theoretical predictions.

Presented in part at the 88th Annual meeting of the American Ceramic Society, Chicago, IL, April 28, 1986 (Paper 75-B-86).

[+]Present address: The University of Missouri-Rolla, Ceramic Engineering Department, Rolla, MO 65401.

[*]Member, the American Ceramic Society.

Supported by the Division of Materials Science, Office of Basic Energy Sciences, U.S. Department of Energy, under Contract No. DE-AC03-76SF00098.

1. INTRODUCTION

It is now widely recognized that inclusions and heterogeneities can have important effects on sintering. Inclusions induce differential sintering rates, which in turn produce transient stresses during sintering.[1] These stresses can not only retard the densification rate of the body but can also induce creep damage by the generation of cracklike voids.[2,3] A number of approaches[1-5] have been used to determine analytically the stresses developed during sintering and their effects on densification. Recently, Scherer[6] has modelled the effect of rigid (i.e. nonsintering, incompressible) inclusions on sintering and has applied the theory to the case of viscous sintering. Scherer considered two models to describe the stresses developed during sintering. First, the composite was represented by a composite sphere, with the core being the inclusion and the cladding being the sintering matrix. This composite sphere model has been used by others[2,3] to consider the same problem, and is expected to apply for low volume fractions of inclusions where the stress fields of the inclusions do not overlap. The second model is related to one used previously to analyze the sintering of a body containing a bimodal pore size distribution.[7] This model, referred to as the self-consistent model, is expected to apply until the volume fraction of inclusions is so great that they form a contiguous network that prevents contraction of the composite. For the case of viscous sintering, the predictions of the two models are indistinguishable for inclusion volume fractions below ~0.2.

Experimentally, the densification of a composite containing rigid, particulate inclusions has been studied by Rahaman and De Jonghe[8] for polycrystalline zinc oxide powder compacts containing different volume fractions of silicon carbide. The main objectives were to investigate the effect of inclusions on the sintering of a polycrystalline oxide system, in

which densification and deformation occur by a diffusion mechanism, and to estimate the transient stresses developed in the matrix due to the constraint of rigid inclusions. In the present study, the investigation of the effect of rigid inclusions on sintering is extended to the case of glass powder compacts in which mass transport occurs by viscous flow.

2. EXPERIMENTAL

A soda-lime glass powder,[+] average particle size ~4μm, was the matrix material, and silicon carbide* particles, classified to a narrow size range with an average of ~35μm, were the inclusion phase. The glass powder was used previously in creep-sintering experiments,[9] and, except for its particle size, the silicon carbide was similar to that used in an earlier study[8] on the effect of inclusions on the sintering of zinc oxide. The powders, containing ~5 v% Carbowax** as binder, were mixed in chloroform and stir-dried, then hand-ground lightly using a mortar and pestle, and finally die-pressed to give composite green compacts (6 mm diameter by 6 mm) having approximately the same matrix density (~0.55) but different volume fractions of inclusions.

The compacts were sintered for 2 hours at 600°C in air, using a dilatometer[10] that allowed the sintering kinetics to be monitored continuously. The binder burnout and sintering procedure was the same as that described previously.[9] The density at any time was determined from the green density and from the measured shrinkage. The final density was also measured using Archimedes' principle. The microstructure of the fracture surface of the sintered compacts was examined in a scanning electron microscope.

[+]Owens-Illinois, Perrysburg, OH 43551

*Geoscience Corp., New York, NY 10175

**Union Carbide Corp., New York, NY 10017

3. DATA ANALYSIS

The experiments give data for the initial density, ρ_{co}, (or the final density, ρ_{cf}) of the composite and the axial shrinkage, $\Delta L/L_o$, of the compact [L_o = initial sample length, and $\Delta L = L_o - L$, where L = instantaneous sample length]. The density of the composite, ρ_c, at any time can be calculated using the relation

$$\rho_c = \rho_{co}(1 - \Delta R/R_o)^{-2}(1 - \Delta L/L_o)^{-1} \quad (1)$$

where R_o is the initial sample radius, and $\Delta R = R_o - R$, where R is the instantaneous sample radius. As observed earlier[8] in the sintering of similar glass powders, the shrinkage is slightly anisotropic, but the axial and radial shrinkages are related by the expression

$$\Delta R/R_o = k\Delta L/L_o \quad (2)$$

where k is a constant for a given experiment. The value of k was obtained from the $\Delta R/R_o$ and $\Delta L/L_o$ values at the end of the sintering experiment. Then

$$\rho_c = \rho_{co}(1 - k\Delta L/L_o)^{-2}(1 - \Delta L/L_o)^{-1} \quad (3)$$

The density of the matrix, ρ_m, at any time is defined as

$$\rho_m = (m_m/V_m) \quad (4)$$

where m_m is the mass, and V_m is the volume of the matrix. If V_{co} and V_c are the initial and instantaneous volumes of the composite, and m_s is the mass, and f_oV_{co} is the volume of the inclusion phase, then

$$\rho_m = (m_c - m_s)/(V_c - f_oV_{co}) \quad (5)$$

where m_c is the total mass of the composite. Taking the density of the inclusion phase as ρ_s, then

$$\rho_m = (\rho_{co}V_{co} - \rho_s f_oV_{co})/(V_c - f_oV_{co}) \quad (6)$$

Since $V_{co}/V_c = \rho_c/\rho_{co}$, then

$$\rho_m = (\rho_{co} - \rho_s f_o)\rho_c/(\rho_{co} - f_o\rho_c) \quad (7)$$

The densification rate of the matrix, $\dot{\rho}_m$, is

$$\dot{\rho}_m = \rho_{co}\dot{\rho}_c(\rho_{co} - f_o\rho_s)/(\rho_{co} - f_o\rho_c)^2 \tag{8}$$

Then, from equations (7) and (8), the volumetric strain rate of the matrix is

$$\dot{\rho}_m/\rho_m = (\dot{\rho}_c/\rho_c)\rho_{co}/(\rho_{co} - f_o\rho_c) \tag{9}$$

The quantity f_o is defined as the volume fraction of the inclusion phase within the initial composite powder compact, which includes the void phase. As the void phase disappears during sintering the volume fraction of the inclusions increase. Usually the volume fraction of the inclusions is calculated on the basis of the fully dense composite, denoted here by F. Then the volume fraction of inclusions, f, at any matrix density, ρ_m, and F are related by the expression

$$f = \rho_m[\rho_m + (1 - F)/F]^{-1} \tag{10}$$

4. RESULTS

Figure 1 shows the density of the composite, ρ_c, versus time, t, for different inclusion volume fractions, F. The results were calculated using equation (3) and the data for the axial shrinkage, $\Delta L/L_o$, which was measured continuously, and the shrinkage anisotropy factor, k, which was measured at the end of each experiment. Each curve is the average of two runs under the same conditions; the results are reproducible to within ±2%. The final density calculated from the sintering curves are in good agreement with the values determined using Archimedes' principle. The beginning of densification was taken as t=0, and the sintering temperature was reached after t=8 minutes. Since the samples were pressed to approximately the same matrix density (~0.51 - 0.55), the increasing initial density of the composite with increasing F reflects the higher density of the silicon carbide inclusions (density ~3.2 Mgm^{-3}) compared with the density of the glass matrix.

The density of the matrix, ρ_m, was calculated from the data of Fig. 1 and equation (7). The theoretical density of the glass was 2.43 Mgm^{-3}, the value measured in earlier experiments.[8] Figure 2 shows the results for ρ_m versus time for different values of F. For $F \leq 0.17$, the initial matrix density was constant at ~0.55, and at any time, the effect of the inclusions on ρ_m is relatively small. Above F ~ 0.17, the samples could not be compacted to the same initial matrix density of 0.55, because of interactions between the rigid inclusion particles; the effect of the inclusions on ρ_m is also seen to be more pronounced.

Since the density of the matrix increases during sintering, the inclusion volume fraction, f, increases with ρ_m (or time). The change in f as a function of ρ_m is shown in Fig. 3 for different values of F. It is seen that f increases approximately linearly with ρ_m.

The composite densification rate, $\dot{\rho}_c/\rho_c$, was found by fitting smooth curves to the data of Fig. 1 and differentiating. Figure 4 shows the results for $\dot{\rho}_c/\rho_c$ versus ρ_m for different values of F. For F=0.09 and for F=0.17 at lower ρ_m, the effect of the inclusions is relatively small, but larger effects become noticeable for F=0.17 at values of $\rho_m \geq 0.8$. The effect of the inclusions is seen to be significant for the sample with F=0.25.

Figure 5 shows a scanning electron micrograph of the fracture surface of a sample with F=0.09 and sintered to a matrix density of ~0.85. The inclusion particle, which is ~10 times the initial particle size of the glass powder, is somewhat angular.

5. DISCUSSION

It is instructive to compare the data of the present study with the predictions of theoretical models. The analysis of Scherer[6] seems well suited to this comparison. Although the predictions of both of Scherer's

models (i.e. the composite sphere model and the self-consistent model) are indistinguishable for viscous sintering with F below ~0.2, the self-consistent model will be used in the present discussion since this model has a greater range of applicability.

According to Scherer's theory, the linear strain rate of the composite, $\dot{\varepsilon}_c$, can be expressed by an equation of the form

$$\dot{\varepsilon}_c = \dot{\rho}_c/(3\rho_c) = (1 - f)K_{s-c}\dot{\varepsilon}_{fm}/(4G_c) \tag{11}$$

where f is the instantaneous volume fraction of inclusions, $\dot{\varepsilon}_{fm}$ is the "free" strain rate of the matrix, and K_{s-c} is related to the "apparent bulk modulus" of the matrix, K_m, and the shear viscosity of the composite, G_c, by

$$K_{s-c} = [1/(4G_c) + f/(3K_m)]^{-1} \tag{12}$$

The rule of mixtures predicts that the linear strain rate of the composite is

$$\dot{\varepsilon}_c^{rm} = (1 - f)\dot{\varepsilon}_{fm} \tag{13}$$

Then from equations (12) and (13),

$$\dot{\varepsilon}_c/\dot{\varepsilon}_c^{rm} = [1 + f(4G_c)/(3K_m)]^{-1} \tag{14}$$

The shear viscosity of the composite, G_c, was taken as the lower bound of the Hashin-Shtrikman equation,[11] and is given by

$$4G_c/(3K_m) = 4G_m/(3K_m)[1 + (15/2)(f/(1 - f))(1 - \nu_m)/(4 - 5\nu_m)] \tag{15}$$

The ratio $4G_m/(3K_m)$ is related to the Poisson's ratio of the matrix, ν_m, by

$$4G_m/(3K_m) = 2(1 - 2\nu_m)/(1 + \nu_m) \tag{16}$$

The Poisson's ratio is related to the matrix density by[12]

$$\nu_m = (1/2)[\rho_m/(3 - 2\rho_m)]^{1/2} \tag{17}$$

Equations (14)-(17) were used to evaluate the theoretical values of $\dot{\varepsilon}_c/\dot{\varepsilon}_c^{rm}$.

In Figure 6, the experimental results for $\dot{\varepsilon}_c/\dot{\varepsilon}_c^{rm}$ are compared with the predictions of equation (14) for values of F of 0.09 and 0.17. It is

seen that the data are in excellent agreement with Scherer's model for F=0.09. For F=0.17, there is initially good agreement with the theory, but significant deviations are evident above ρ_m~0.7. At this value of ρ_m, the inclusion volume fraction, f, is ~0.12. The deviations from the theory for F=0.25 are very large and fall outside the scale of Figure 6. One factor which may give rise to the large deviations between theory and experiment above f~0.12 is interaction between the inclusion particles. Scherer's model does not allow for the fact that the inclusions will initially interfere, and later will come into contact and stop densification at some critical volume fraction, f*. For inclusions of uniform size, percolation theory[13] indicates that the inclusion will form a contiguous network when f~0.16. Since Figure 2 indicates that appreciable densification occurs for much higher values of f, it appears that the inclusion network is not stiff enough to resist the sintering stress. For angular inclusion particles (Figure 5), the value of f at which significant deviations from theory become evident would be expected to be slightly smaller than for spherical particles. Figure 6 also shows that the deviation from the rule of mixtures is ≤5% for F≤0.1.

The stresses caused by the inclusions in the sample can also be calculated. According to Scherer's model, the ratio of the hydrostatic stress, σ_m, in the matrix caused by the inclusions, to the sintering stress, Σ, is given by

$$\sigma_m/\Sigma = -f[f + 3K_m/(4G_c)]^{-1} \tag{18}$$

Thus σ_m/Σ can be evaluated using equations (16) and (17). The shear stress at the interface between the inclusion and the matrix is given by

$$\sigma_i = -(1 - f)\sigma_m/f \tag{19}$$

The experimental values for σ_m/Σ can be determined by recalling that the effective sintering stress in the matrix is related to the "free" strain rate by

$$3\dot{\varepsilon}_m = -3\dot{\varepsilon}_{fm}(1 - \sigma_m/\Sigma) \tag{20}$$

Figure 7 shows a comparison between the experimental and theoretical values for σ_m/Σ as a function of ρ_m, for F=0.09 and F=0.17. As observed earlier for the $\dot{\varepsilon}_c/\dot{\varepsilon}_c^{rm}$ results, the experimental data show excellent agreement with Scherer's model for F≤0.12. For F≤0.1, the maximum value of σ_m/Σ is quite small, i.e. ≤0.05, and thus cannot lead to any appreciable deviations from the rule of mixtures (Figure 6). The experimental and theoretical data for σ_i/Σ, plotted as a function of ρ_m, is shown in Figure 8 for F=0.09. The experimental data is seen to be in excellent agreement with Scherer's theory. As shown earlier, strong deviations from theory occur for f≥0.12, and these data have been omitted. Figure 8 shows that σ_i is a significant fraction of the sintering stress in the early stages of densification, but its value is not nearly as great as the σ_i values obtained for polycrystalline matrices,[3,7] where σ_i has been estimated as many times larger than the sintering stress.

6. CONCLUSIONS

The effect of rigid inclusions on the sintering of glass has been investigated, and the stresses caused by the inclusions during sintering have been calculated and compared with Scherer's theory of viscous sintering with rigid inclusions. The densification rates are in good agreement with the rule of mixtures for inclusion volume fractions of ≤0.1. The data for the densification rates, and the stresses caused by the inclusions are in excellent agreement with Scherer's theory for inclusion volume fractions of ≤0.12. Above this value, interactions between the inclusions cause significant deviations from theory. The results suggest

that high density composites can be fabricated readily by conventional (pressureless) sintering for inclusion volume fractions of ≤ 0.15 provided that the matrix deforms in a viscous manner.

Acknowledgement: The authors thank Dr. G.W. Scherer for a preprint of his paper (Reference 6).

REFERENCES

1. A.G. Evans, "Considerations of Inhomogeneity Effects in Sintering," J. Am. Ceram. Soc., 65 [10] 497-501 (1982).
2. R. Raj and R.K. Bordia, "Sintering Behavior of Bimodal Compacts," Acta Metall., 32 [7] 1003-1019 (1984).
3. C.H. Hsueh, A.G. Evans, R.M. Cannon, and R.J. Brook, "Viscoelastic Stresses and Sintering Damage in Heterogeneous Powder Compacts," Acta Metall., 34 [5] 927-936 (1986).
4. C.H. Hsueh, A.G. Evans, and R.M. McMeeking, "Influence of Multiple Heterogeneities on Sintering Rates," J. Am. Ceram. Soc., 69 [4] C64-C66 (1986).
5. L.C. De Jonghe and M.N. Rahaman, "Sintering Stress of Homogeneous and Heterogeneous Powder Compacts," submitted to Acta Metall.
6. G.W. Scherer, "Sintering with Rigid Inclusions," submitted to J. Am. Ceram. Soc.
7. G.W. Scherer, "Viscous Sintering of a Bimodal Pore Size Distribution," J. Am. Ceram. Soc., 67 [11] 709-715 (1984).
8. L.C. De Jonghe, M.N. Rahaman, and C.H.Hsueh, "Transient Stresses in Bimodal Compacts During Sintering," Acta Metall., 34 [7] 1467-1471 (1986).
9. M.N. Rahaman, L.C. De Jonghe, G.W. Scherer, and R.J. Brook, "Creep and Densification During Sintering of Glass Powder Compacts," submitted to J. Am. Ceram. Soc.
10. L.C. De Jonghe and M.N. Rahaman, "A Loading Dilatometer," Rev. Sci. Instrum, 55 [12] 2007-2010 (1984).

11. Z. Hashin and S. Shtrikman, "A Variational Approach to the Theory of the Elastic Behavior of Multiphase Materials," J. Mech. Phys. Solids, 11 127-140 (1963).

12. G.W. Scherer, "Sintering of Inhomogeneous Glasses: Application to Optical Waveguides," J. Non-Crystalline Solids, 34 239-256 (1979).

13. R. Zallen, The Physics of Amorphous Solids, pp. 183-186, Wiley, NY, 1983.

LIST OF FIGURES

1. Density of the composite, ρ_c, versus time, for indicated volume fractions of inclusions, F.

2. Relative density of the matrix, ρ_m, versus time, for indicated volume fractions of inclusions, F.

3. Instantaneous volume fraction of inclusions, f, versus relative density of the matrix, ρ_m, for indicated volume fractions of inclusions, F.

4. Volumetric strain rate of the composite, $\dot{\rho}_c/\rho_c$, versus relative density of the matrix, ρ_m, for indicated volume fractions of inclusions, F.

5. Scanning electron micrograph of the fracture surface of a sample with a volume fraction of inclusions, F, of 0.09 and sintered to a relative matrix density, ρ_m, of ~0.85.

6. Comparison of the experimental results for the linear strain rate of the composite normalized by the strain rate from the rule of mixtures [equation (13)], $\dot{\varepsilon}_c/\dot{\varepsilon}_c^{rm}$, versus relative density of the matrix, ρ_m, with the predictions of Scherer's model [equation (14)], for indicated volume fractions of inclusions, F.

7. Hydrostatic stress in the matrix normalized to the sintering stress [equation (20)], σ_m/Σ, versus the relative density of the matrix, ρ_m, compared with the predictions of Scherer's theory, [equation (18)], for indicated volume fractions of inclusions, F.

8. Shear stress at the interface normalized to the sintering stress, [equation (19)], σ_i/Σ, versus the relative density of the matrix, ρ_m, compared with the predictions of Scherer's theory for volume fraction of inclusions, F, of 0.09.

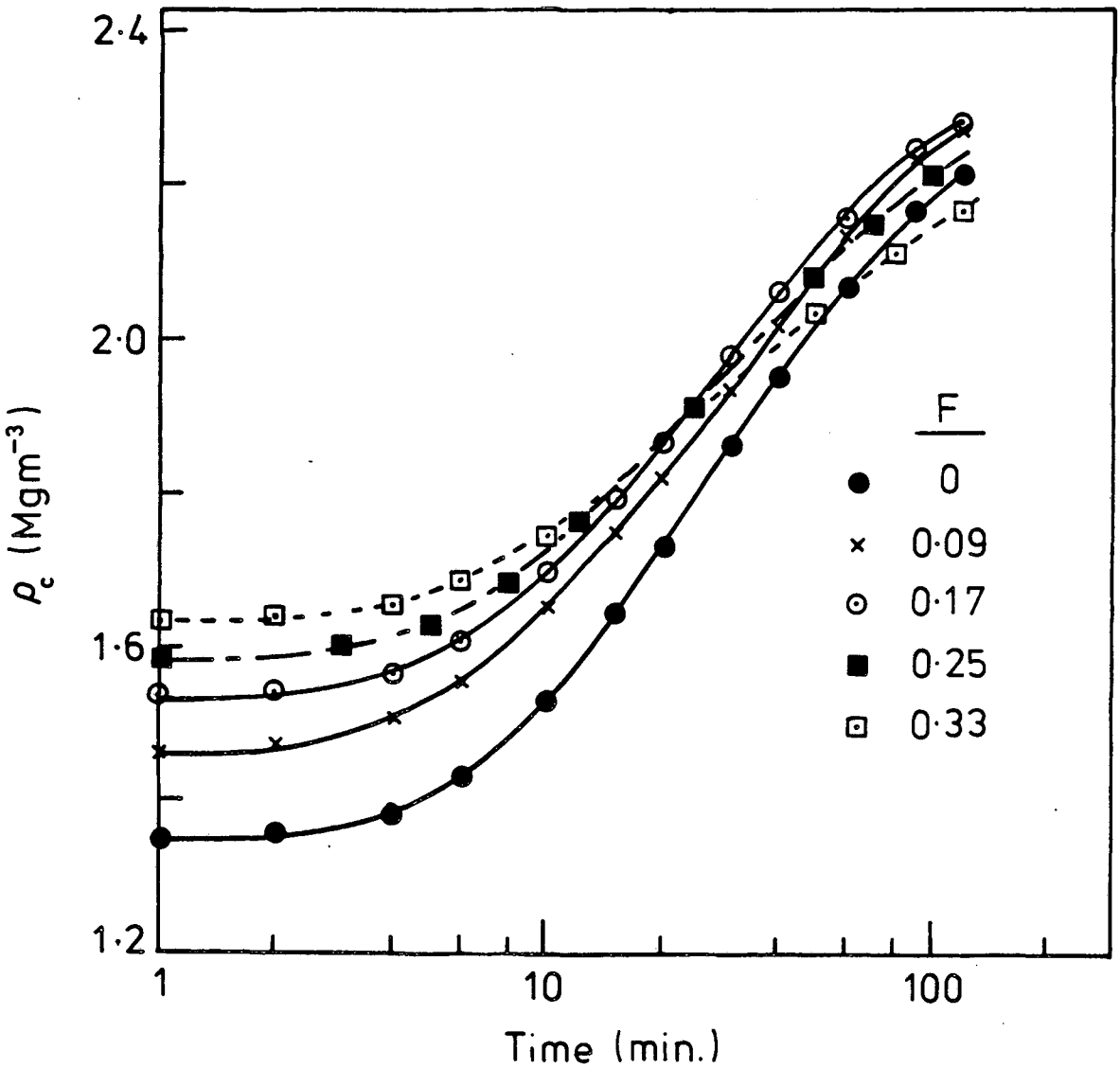

XBL 874-1749

Fig. 1

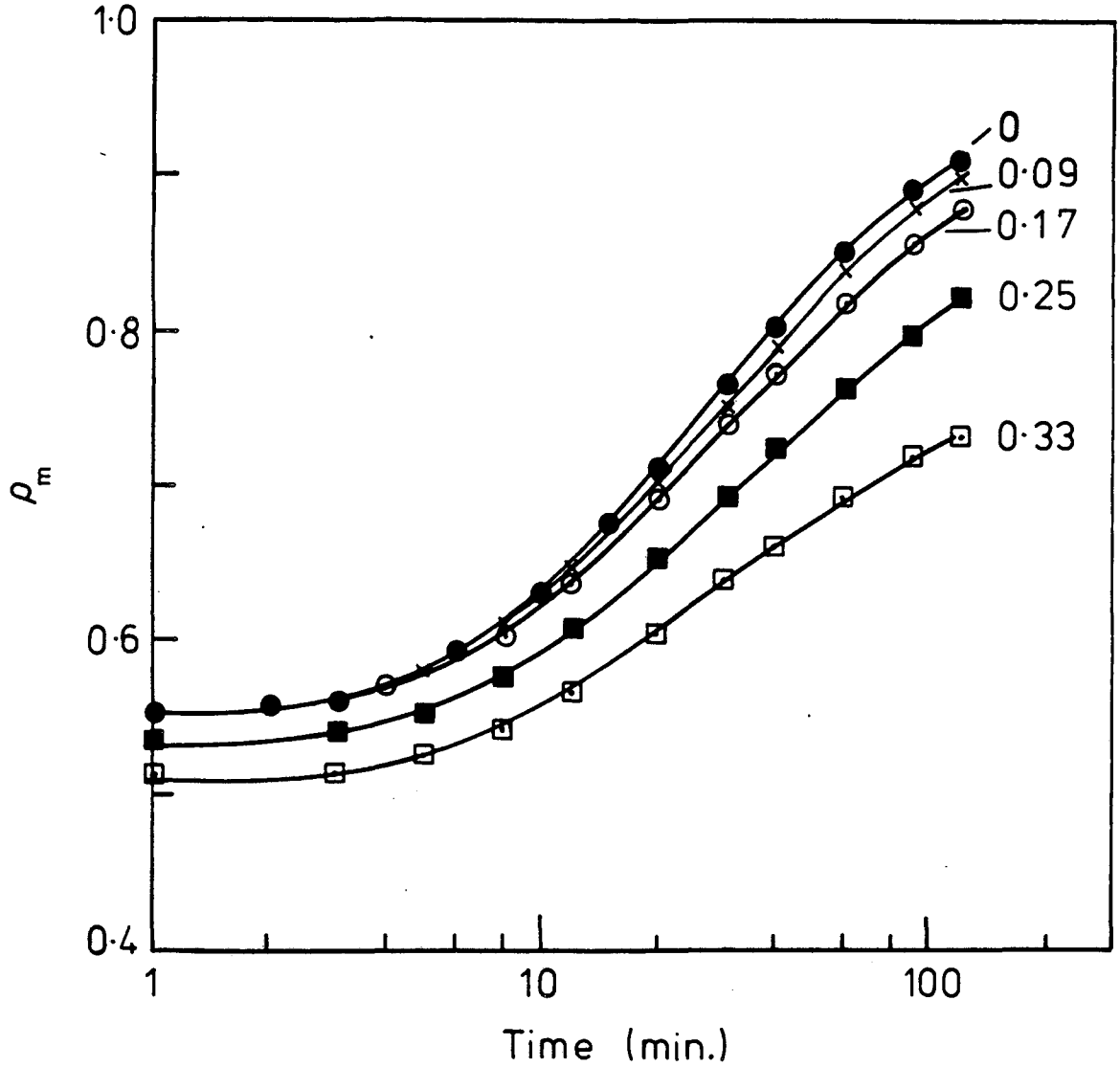

XBL 874-1748

Fig. 2

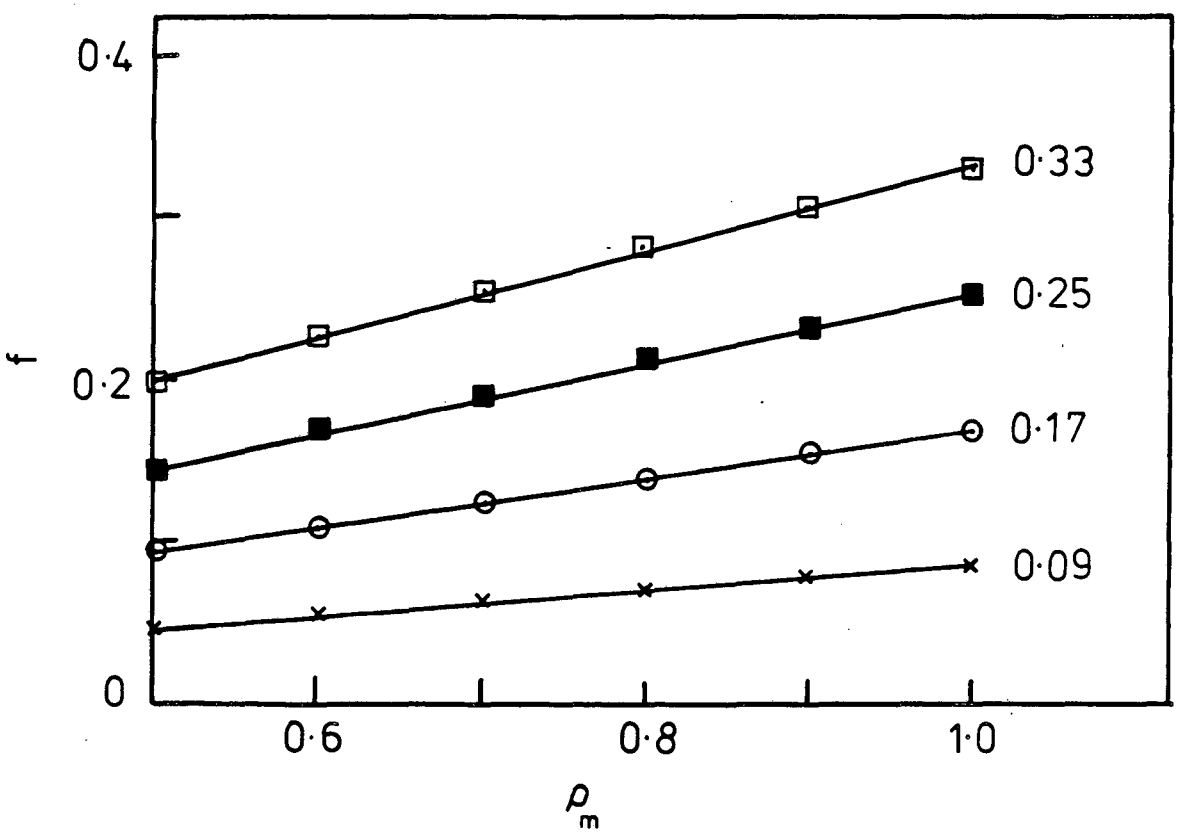

XBL 874-1747

Fig. 3

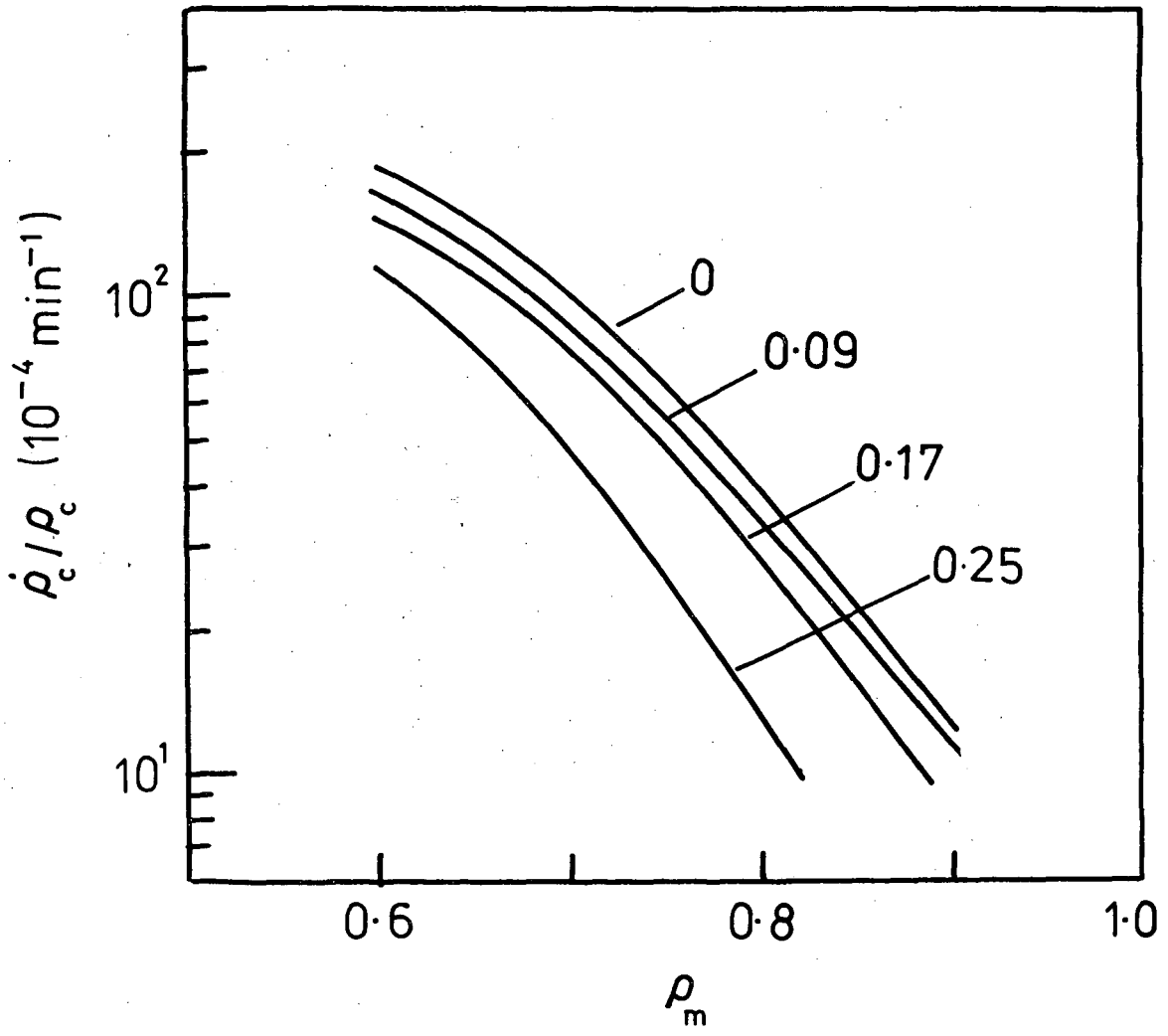

XBL 874-1746

Fig. 4

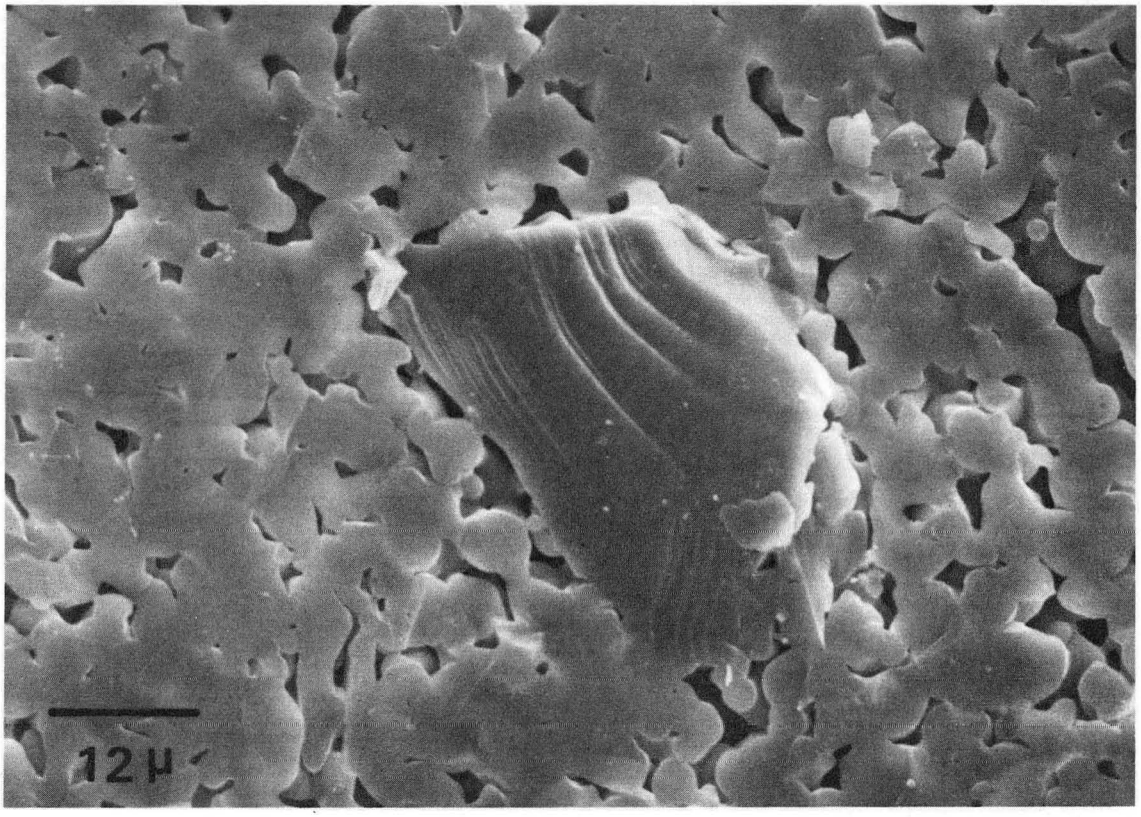

XBB850-8635

Fig. 5

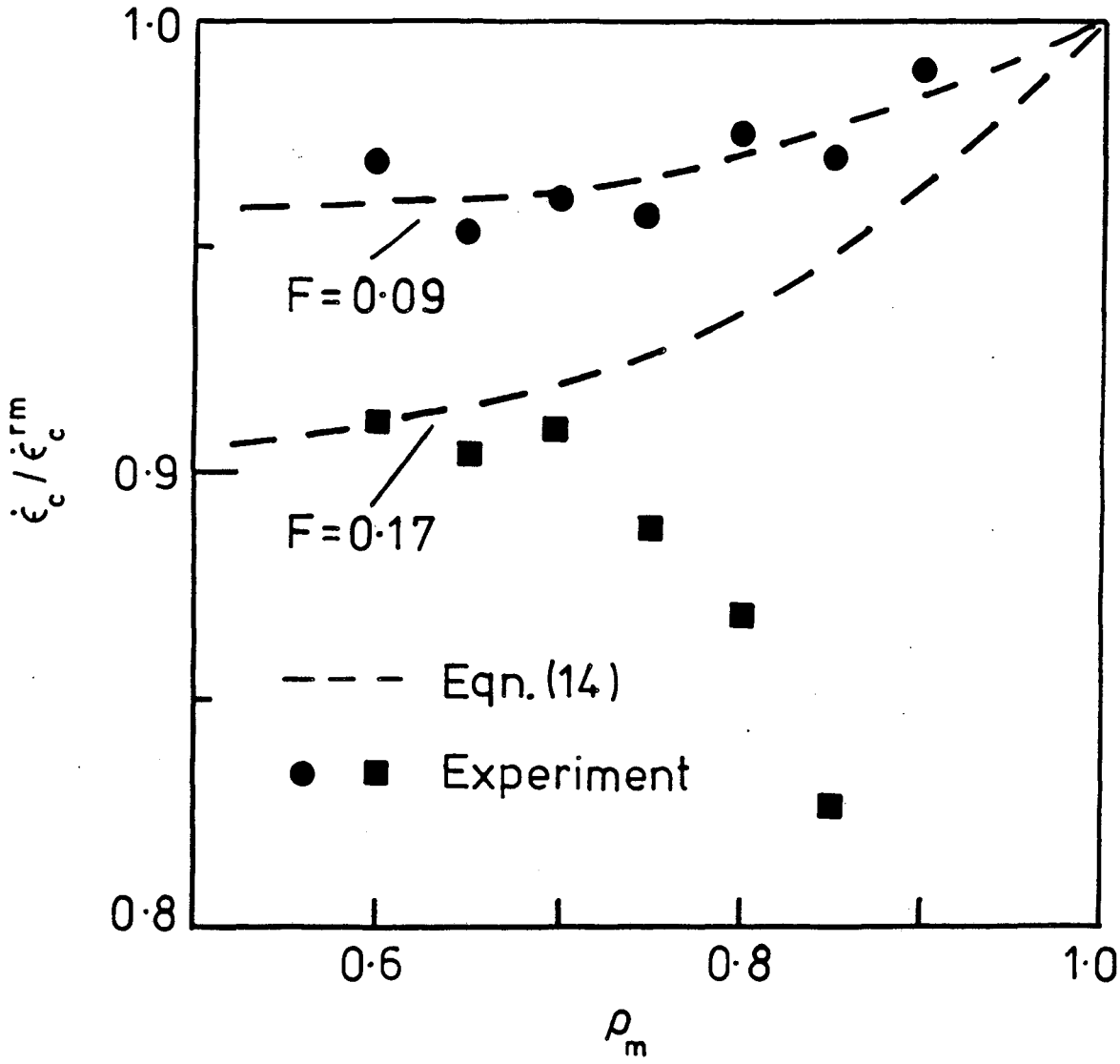

XBL 874-1745

Fig. 6

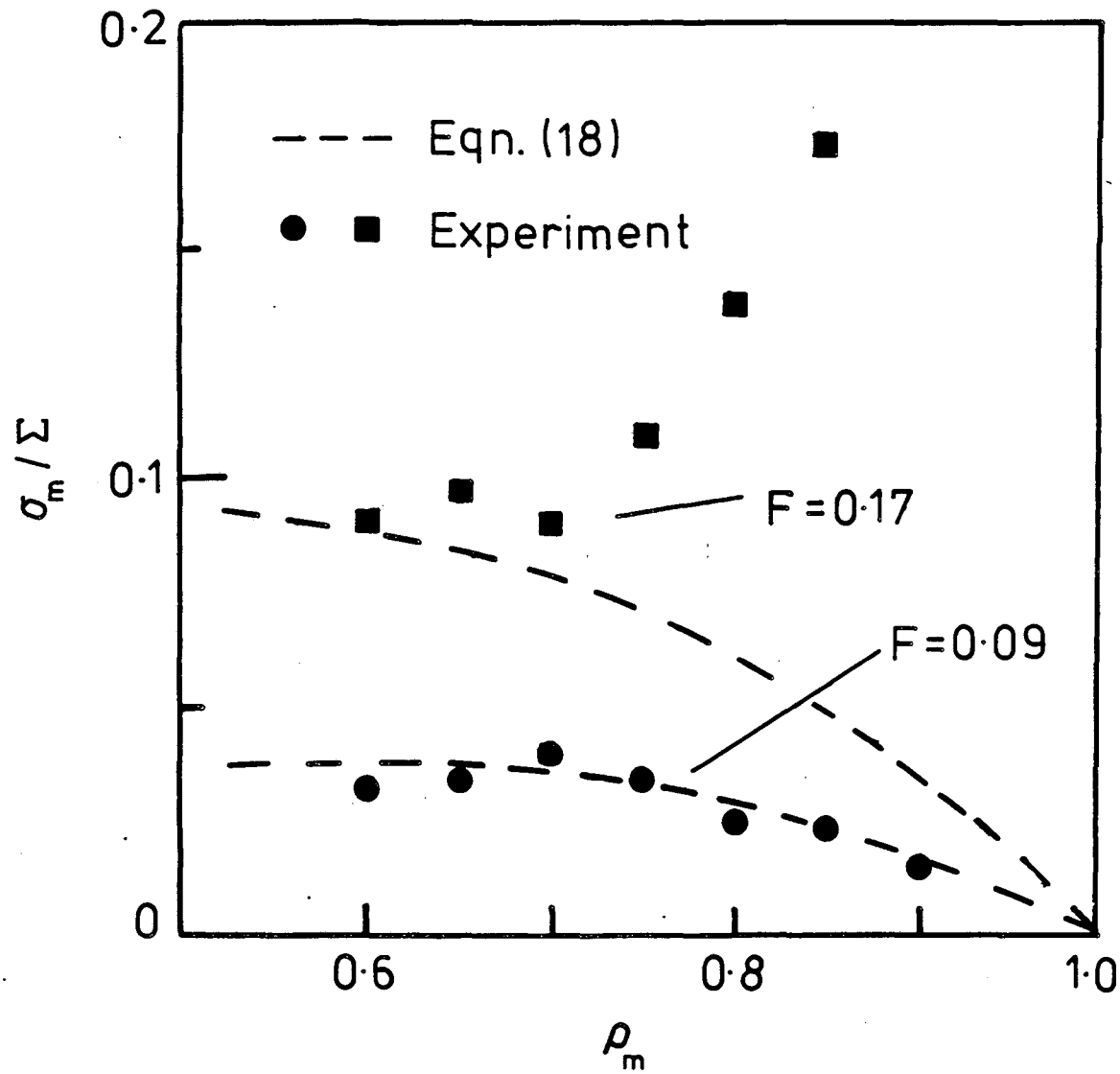

XBL 874-1744

Fig. 7

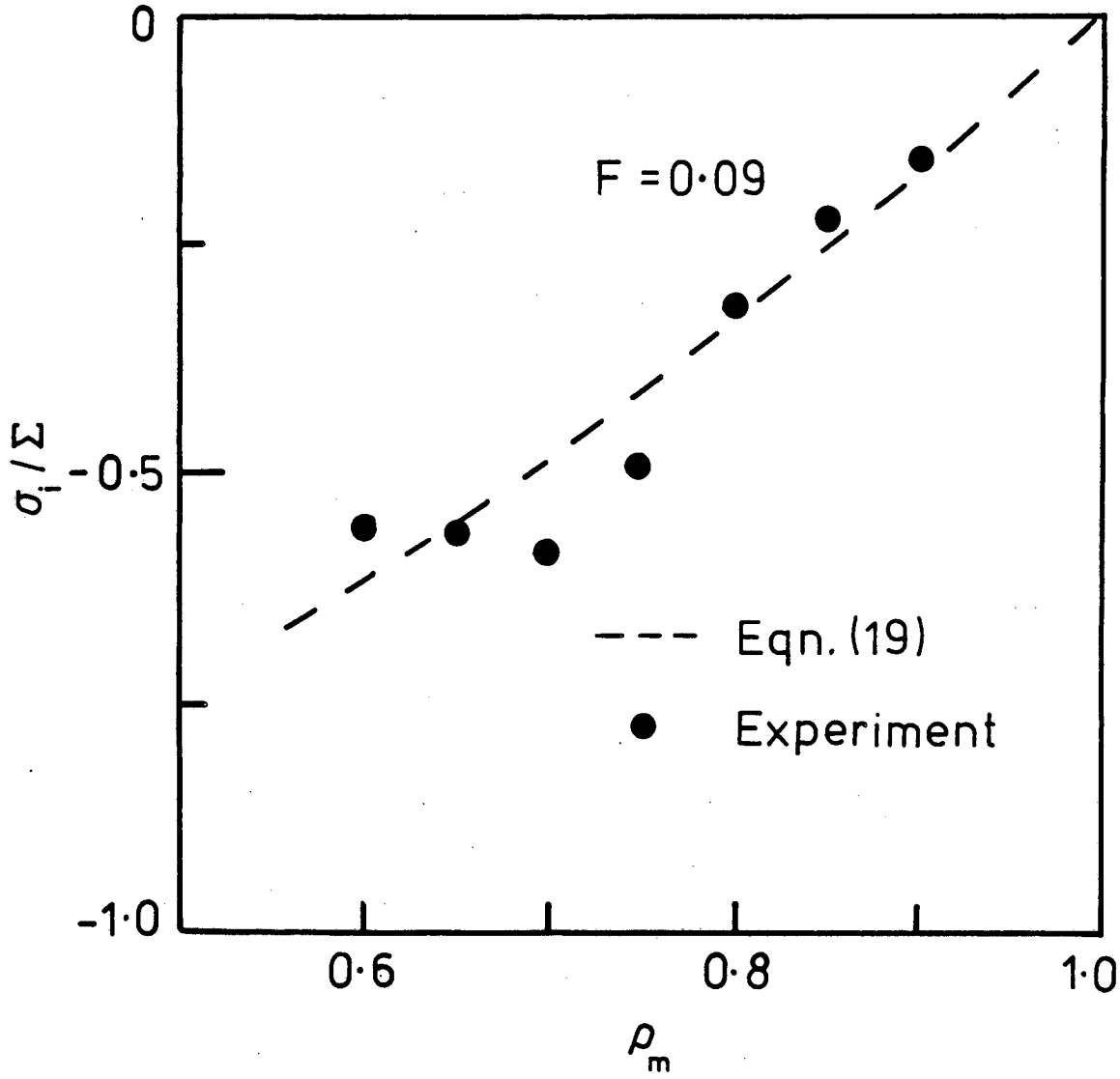

XBL 874-1743

Fig. 8

This report was done with support from the Department of Energy. Any conclusions or opinions expressed in this report represent solely those of the author(s) and not necessarily those of The Regents of the University of California, the Lawrence Berkeley Laboratory or the Department of Energy.

Reference to a company or product name does not imply approval or recommendation of the product by the University of California or the U.S. Department of Energy to the exclusion of others that may be suitable.

LAWRENCE BERKELEY LABORATORY
TECHNICAL INFORMATION DEPARTMENT
UNIVERSITY OF CALIFORNIA
BERKELEY, CALIFORNIA 94720